

Supplement of The Cryosphere, 14, 633–656, 2020
<https://doi.org/10.5194/tc-14-633-2020-supplement>
© Author(s) 2020. This work is distributed under
the Creative Commons Attribution 4.0 License.



Supplement of

Glacial-cycle simulations of the Antarctic Ice Sheet with the Parallel Ice Sheet Model (PISM) – Part 2: Parameter ensemble analysis

Torsten Albrecht et al.

Correspondence to: Torsten Albrecht (albrecht@pik-potsdam.de)

The copyright of individual parts of the supplement might differ from the CC BY 4.0 License.

Supplementary Material S1: Ensemble of basal parameters

In the sensitivity analysis of various parameters and boundary conditions in a companion paper (Albrecht et al., 2019), we
745 found that the basal sliding parameterization in conjunction with the sub-glacial hydrology scheme show very diverse simulated ice volume histories for a plausible range of unconfined parameter values. We have chosen the parameter PPQ (Sect. 3.1) as only representative of basal processes uncertainties for the ensemble analysis.

Here we want to span a sub-ensemble including three other relevant basal parameters. The four parameters and sampled
750 values used in the basal ensemble analysis are:

- *PHIMIN* is the minimal till friction angle on the continental shelf, mainly underneath modern ice shelves, where sandy sediments are prevalent (friction coefficient on the continental shelf has been chosen as one of the ensemble parameters in Pollard et al. (2016, 2017)). The tangens of till friction angle enters the Mohr-Coulomb-yield stress criterion. Sampled values are 0.5° , 1° , 2° and 3° .
- 755 – *TWDR* is the decay rate of the effective water content within the till layer using the non-conserving hydrology model, while basal melt adds water up to a certain threshold (for details see Bueler and van Pelt, 2015, Sect. 3.1). Sampled value are 0.5 mm yr^{-1} ($1.55 \times 10^{-11} \text{ m s}^{-1}$), 1 mm yr^{-1} ($3.1 \times 10^{-11} \text{ m s}^{-1}$), 5 mm yr^{-1} ($15.5 \times 10^{-11} \text{ m s}^{-1}$) and 10 mm yr^{-1} ($31 \times 10^{-11} \text{ m s}^{-1}$).
- *FEOP* is the fraction of the effective overburden pressure (for details see Bueler and van Pelt, 2015, Sect. 3.2), for which
760 excess water will be drained into a transport system in the case of saturated till. Sampled values are 1%, 2%, 4%, 8% and 32%.
- *PPQ* is the sliding exponent as in the ensemble (see Sect. 3.1)

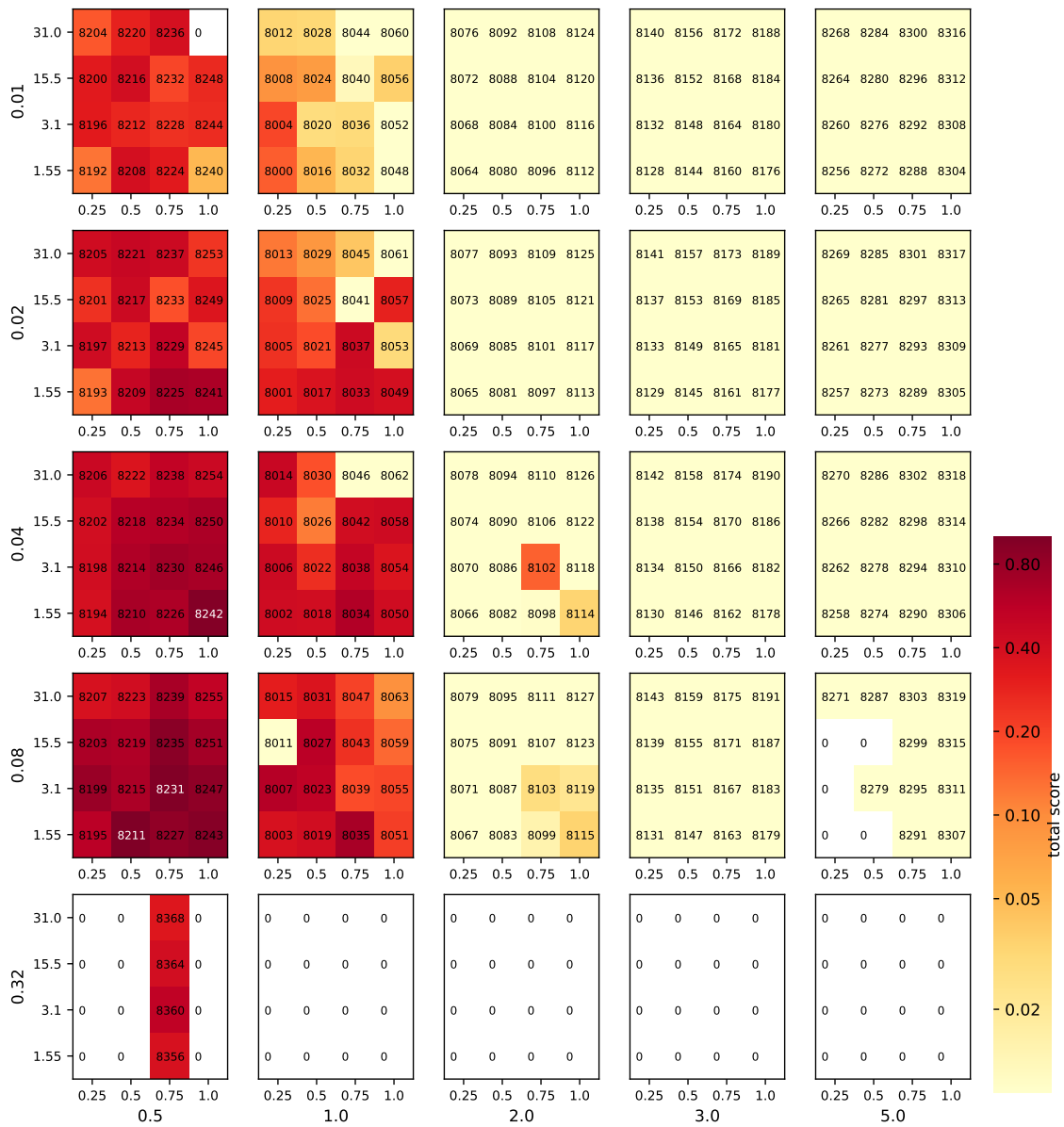


Figure S1. Aggregated score for 318 ensemble members (4 model parameters, 4-5 values each) showing the distribution of the scores over the full range of plausible basal parameter values. The score values are computed versus geologic and modern data sets, normalized by the best score in the ensemble, and range from <0.01 (bright yellow, no skill) to 1 (dark red, best score) (cfs. Pollard et al., 2016, Figs. 2 + C1), on a logarithmic color scale. The four parameters are the effective overburden pressure fraction FEOP (outer y-axis), the minimal till friction angle on the continental shelf PHIMIN (outer x-axis), the tillwater decay rate TWDR (inner y-axis) and the power-law sliding pseudoplasticity exponent PPQ (inner x-axis). In the lowest row, only four ensemble scores are shown for 32% of effective overburden pressure fraction, just to ascertain that aggregated scores decline for larger FEOP.

In the basal sub-ensemble we find even better scores than for the best fit parameter combination in the base ensemble (here no. 8102, see Fig. S1) that covers also climatic, Earth and ice-internal parameters. Best scores are found in particular for smaller minimal till friction angles $PHIMIN = 0.5-1^\circ$, but also for rather high values of the fraction of the effective overburden pressure at which excess water drains, here $FEOP = 4-16\%$. These values are higher than those used in the base ensemble. However, best fit to the nine data constraints are found for the basal ensemble in the middle range of $PPQ = 0.5-0.75$ and the lower range of till water decay rates of $TWDR = 0.5-1.0 \text{ mm yr}^{-1}$ ($1.55-3.1 \times 10^{-11} \text{ m s}^{-1}$), which agrees with the best fit parameter combination of the base ensemble ($PPQ=0.75$ and $TWDR=1.0 \text{ mm yr}^{-1}$). The LGM volume of the best fit simulation of the basal ensemble is considerably smaller (4.5 m SLE) than in the best fit simulation of the base ensemble (cf. Figs. S2 and 15), and deglacial retreat occurs a few thousand years earlier for lower $PHIMIN$ (Fig. S3).

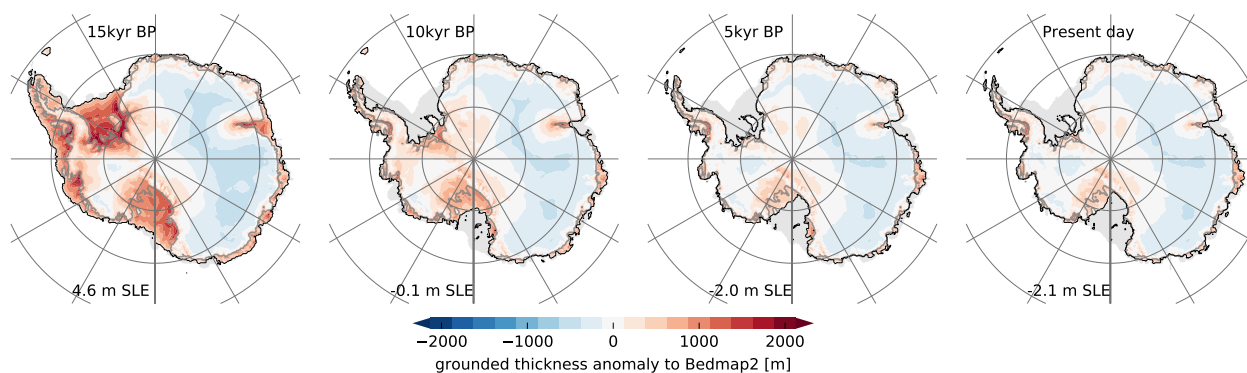


Figure S2. Snapshots of grounded ice thickness anomaly to present-day observations (Bedmap2; Fretwell et al., 2013) over the last 15 kyr for best-fit simulation in the basal ensemble. At LGM state grounded ice extends towards the edge of the continental shelf, with much thicker ice than present mainly in West Antarctica. Retreat of the ice sheet initiates between 12 and 11 kyr BP and halts already latest 8 kyr in all large ice shelf basins of Ross, Weddell Sea, Amery and Amundsen Sea. East Antarctic Ice Sheet thickness is underestimated throughout the deglaciation period (light blue). Compare Fig. 2 in Golledge et al. (2014).

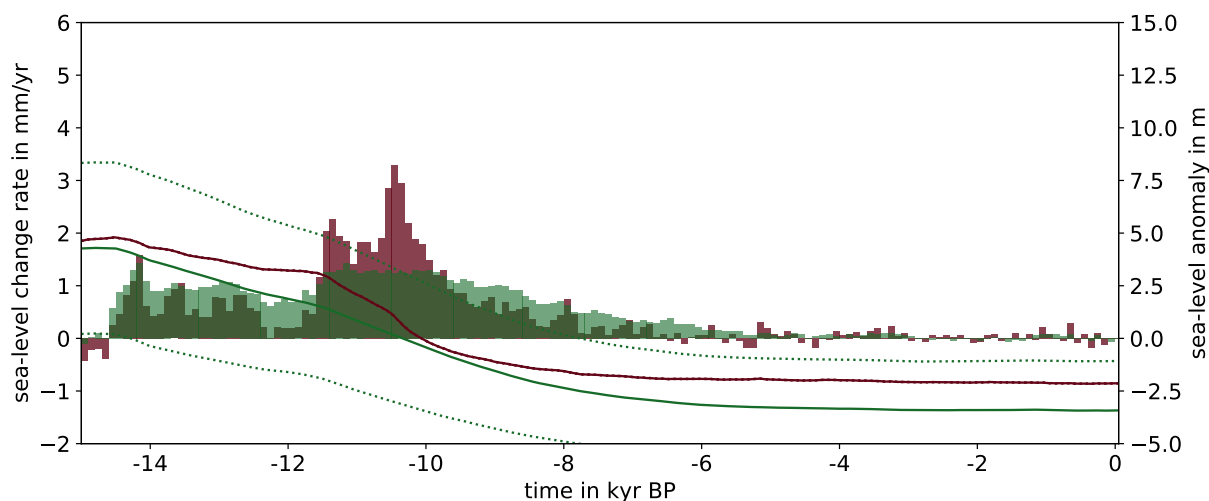


Figure S3. During deglaciation the score-weighted ensemble mean (green) shows most of the sea-level change rates between 14.5 kyr BP (MWP1a) and 8 kyr BP with mean rates around 1 mm yr^{-1} , while the best-score simulation (red) reveals rates of sea-level rise of up to 4 mm yr^{-1} (100-yr bins) in the same period (cf. Gollidge et al., 2014, Fig. 3 d). In contrast to the base ensemble (see Fig. 9c) the basal ensemble shows a much earlier deglacial retreat and no regrowth during the late Holocene.

Supplementary Material S2: Misfit to individual paleo data types

This supplement compares model results with corresponding geological data types (AntICEdat from Briggs and Tarasov
 775 (2013)) used in the ensemble scoring. This absolute misfit is important information as all scores are normalized against their median (relative fit) in order to calculate the aggregated scores. Thereby, we want to demonstrate how well the ensemble simulations span the data constraints and hence potentially represent reasonably realistic ice-sheet behavior.

Fig. S4 compares elevation vs. age for all 256 runs with cosmogenic data at 26 sites (ELEV; Briggs and Tarasov, 2013) with
 780 a median age of constraint of 9.6 kyr. We find a good fit in parts of East Antarctica (e.g. Framnes Mts. (1201-1203)) and in parts of the Ross sector (e.g. Clark Mts. (1405), Allegheny Mts. (1406) or Eastern Fosdick Mts. (1408)), while in the West Antarctic Ice Sheet there is quite a large spread among the ensemble misfit of up to 1,000 m in surface elevation, with ensemble mean misfits of up to 1,000 m. This is due to the fact that in many ensemble simulations the large ice shelves of Ronne-Filchner, Ross and Amery do not become afloat in time, while the best-fit simulation (green markers) shows quite a good fit, although some regions remain thicker than observed until present (Fig. 12).

785 Fig. S5 shows the misfit of simulated grounding lines retreat for all ensemble simulations at 27 marine core sites (EXT; Briggs and Tarasov, 2013), which are relatively well distributed around the Antarctic Ice Sheet with a median age of 16.6 kyr, the oldest data point 30.7 kyr. Generally, simulated grounding-line retreat occurs later than in most of the observations, less than 5 kyr near Victoria Land, Ross Sea and along the Antarctic Peninsula (2303, 2402-2403, 2602-2608) and less than 10 kyr

790 in the Amundsen Sea, and Weddell Sea (2502, 2609, 2701). At some locations (Dronning Maud-Enderby Land (2101-2103)
or at Victoria Land (2304)), however, the ensemble never reproduces the recorded open ocean conditions or grounding-line
retreat event, respectively.

795 Although not used as constraint in our scoring scheme, Fig. S7 shows the misfit of modelled relative sea level in all ensemble
simulations with respect to 96 RSL proxy records at eight sites (RSL; Briggs and Tarasov, 2013), with a median age of 5.0 kyr.
The data for each site fall well within the overall model envelope (upper and lower bound indicated) with best fits at Syowa
Coast (9101), Larsemann Hills (9201), Vestfold Hills (9202), Windmill Islands (9301), and Marguerite Bay (9601) and King
George Island (9602), while in Victoria Land the model ensemble generally overestimates regional sea level (Terra Nova Bay
(9401) and Southern Scott Coast (9402)).

800 From each data type misfit we obtain an ensemble distribution of misfits (Fig. S6), which can be rather normal (e.g. for
EXT), exponential (e.g. TOTUPL) or long-tail (e.g. TOTDH). In order to calculate aggregated scores we normalize by the
median value, which yields for most data types similar results as the mean value, except for TROUGH (34% difference). The
corresponding variability of each of the resultant normalized scores hence contribute different skills to the aggregated score.
Generally, grounding-line related (TOTE, TOTGL, THROUGH) and ice volume-related data-types (TOTDH) show similar
individual score patterns (not shown here) with ensemble standard deviations of 0.1-0.2. In the aggregated score this patterns
becomes even more pronounced, while paleo scores (ELEV and EXT) and ice shelf extent (TOTI) show only little variation
805 (<0.1) among the ensemble, and hence only little effect in the aggregate score pattern.

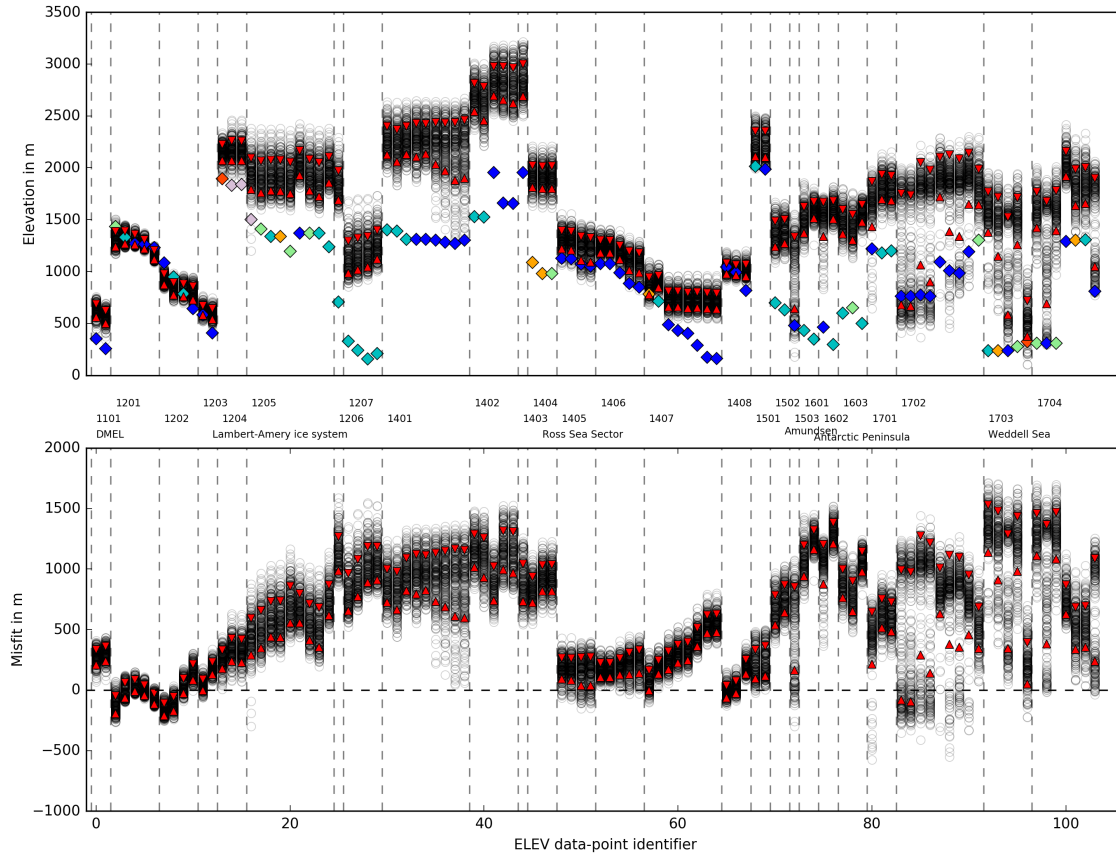


Figure S4. ELEV observations (colored diamonds, dark and light blue indicate last 10 kyr or 20-10 kyr observational interval) taken from database by Briggs and Tarasov (2013), ensemble results (black circles), upper and lower bounds from base ensemble (red triangles), and computed misfits (lower panel) for different Antarctic Peninsula sectors, indicated by vertically dashed lines and labels between panels. Green dots correspond to best-fit simulation. Compare to Fig. 7–9 for in Briggs et al. (2014) with same data-point identifiers.

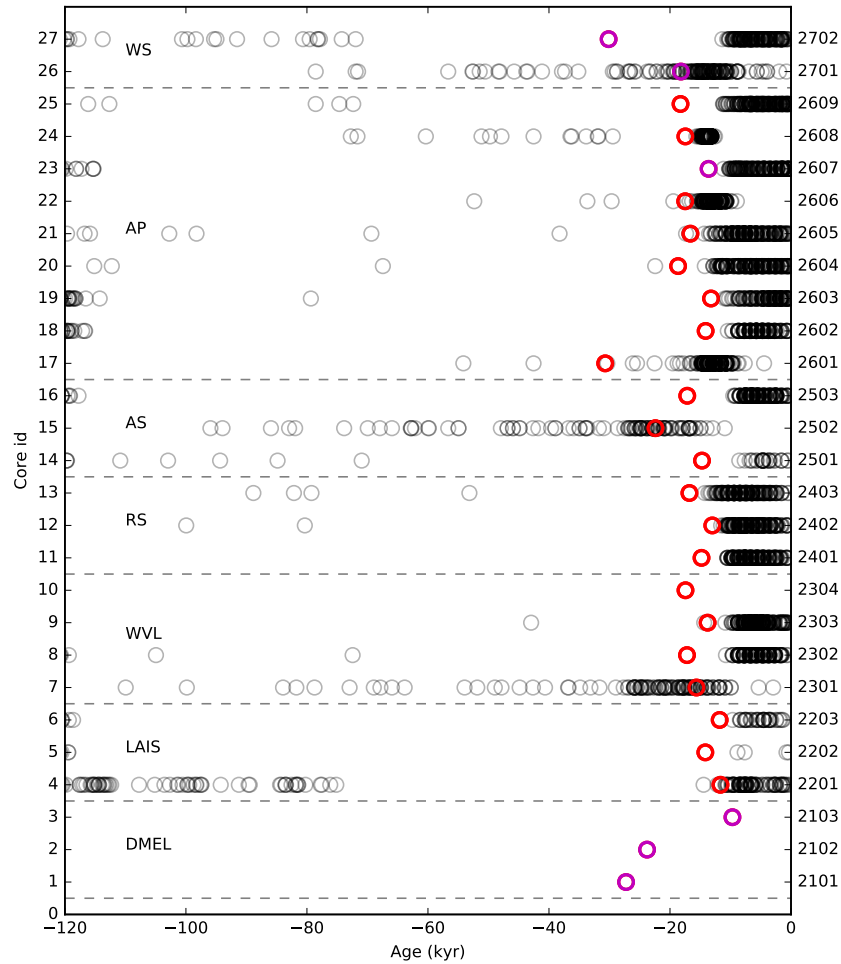


Figure S5. EXT observations and ensemble results as in Fig. 10 in Briggs et al. (2014). Black circles represent the 256 ensemble simulations with the best-fit simulation in green. Red indicate the grounding-line retreat (GLR) two-way constraint types, magenta the open marine conditions (OMC) one-way constraint types. Dashed horizontal lines and associated labels segregate and identify the different sectors.

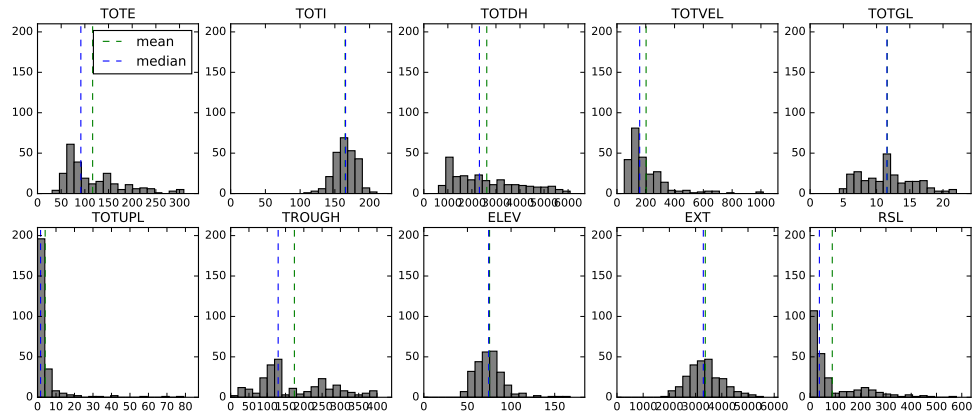


Figure S6. Histogram of misfits per data-type with median (in blue) and mean (green).

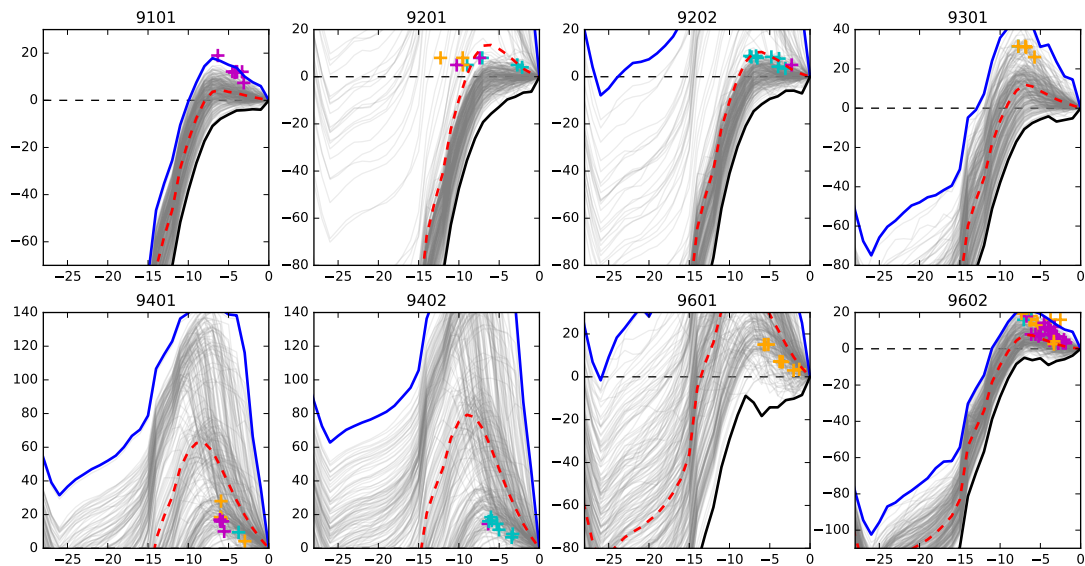


Figure S7. Regional sea level (RSL) data points and ensemble sea level curves for the 8 data sites, analogous to Fig. 5–6 in Briggs et al. (2014), upper panels in EAIS, lower panels in Antarctic Peninsula and Ross sector. Observed RSL data points are colour coded according to the constraint they provide: two-way (light blue, dated past sea level); one-way lower-bounding (mauve, past sea level above or maximum age of beach) or one-way upper-bounding (orange, past sea level below or minimum age beach). For a detailed description of the RSL datasets and its processing, refer to Briggs and Tarasov (2013). RSL has not been used as constraint in this study.

References

- Albrecht, T., Winkelmann, R., and Levermann, A.: Glacial cycles simulation of the Antarctic Ice Sheet with PISM - Part 1: Boundary conditions and climatic forcing, *The Cryosphere Discussions*, 2019, <https://doi.org/10.5194/tc-2019-71>, <https://www.the-cryosphere-discuss.net/tc-2019-71/>, 2019.
- 810 Briggs, R., Pollard, D., and Tarasov, L.: A glacial systems model configured for large ensemble analysis of Antarctic deglaciation, *The Cryosphere*, 7, 1949–1970, 2013.
- Briggs, R. D. and Tarasov, L.: How to evaluate model-derived deglaciation chronologies: a case study using Antarctica, *Quaternary Science Reviews*, 63, 109–127, 2013.
- Briggs, R. D., Pollard, D., and Tarasov, L.: A data-constrained large ensemble analysis of Antarctic evolution since the Eemian, *Quaternary Science Reviews*, 103, 91–115, <https://doi.org/10.1016/j.quascirev.2014.09.003>, 2014.
- 815 Bueler, E. and van Pelt, W.: Mass-conserving subglacial hydrology in the Parallel Ice Sheet Model version 0.6, *Geoscientific Model Development*, 8, 1613, 2015.
- Fretwell, P., Pritchard, H. D., Vaughan, D. G., Bamber, J. L., Barrand, N. E., Bell, R., Bianchi, C., Bingham, R. G., Blankenship, D. D., Casassa, G., Catania, G., Callens, D., Conway, H., Cook, A. J., Corr, H. F. J., Damaske, D., Damm, V., Ferraccioli, F., Forsberg, R., Fujita, S., Gim, Y., Gogineni, P., Griggs, J. A., Hindmarsh, R. C. A., Holmlund, P., Holt, J. W., Jacobel, R. W., Jenkins, A., Jokat, W., Jordan, T., King, E. C., Kohler, J., Krabill, W., Riger-Kusk, M., Langley, K. A., Leitchenkov, G., Leuschen, C., Luyendyk, B. P., Matsuoka, K., Mouginot, J., Nitsche, F. O., Nogi, Y., Nost, O. A., Popov, S. V., Rignot, E., Rippin, D. M., Rivera, A., Roberts, J., Ross, N., Siegert, M. J., Smith, A. M., Steinhage, D., Studinger, M., Sun, B., Tinto, B. K., Welch, B. C., Wilson, D., Young, D. A., Xiangbin, C., and Zirizzotti, A.: Bedmap2: improved ice bed, surface and thickness datasets for Antarctica, *The Cryosphere*, 7, 375–393, <https://doi.org/10.5194/tc-7-375-2013>, <https://secure.antarctica.ac.uk/data/bedmap2/>, 2013.
- 825 Golledge, N. R., Menviel, L., Carter, L., Fogwill, C. J., England, M. H., Cortese, G., and Levy, R. H.: Antarctic contribution to meltwater pulse 1A from reduced Southern Ocean overturning, *Nature Communications*, 5, <https://doi.org/10.1038/ncomms6107>, 5107, 2014.
- Pollard, D., Chang, W., Haran, M., Applegate, P., and DeConto, R.: Large ensemble modeling of the last deglacial retreat of the West Antarctic Ice Sheet: comparison of simple and advanced statistical techniques, *Geosci. Model Dev.*, 9, 1697–1723, <https://doi.org/10.5194/gmd-9-1697-2016>, 2016.
- 830